Hypothesis

Kinetic model of ATP synthase: pH dependence of the rate of ATP synthesis

Siddhartha Jain, Sunil Nath*

Department of Biochemical Engineering and Biotechnology, Indian Institute of Technology, Hauz Khas, New Delhi 110 016, India

Received 19 May 2000

Edited by Matti Saraste

Abstract Recently, a novel molecular mechanism of torque generation in the F_0 portion of ATP synthase was proposed [Rohatgi, Saha and Nath (1998) Curr. Sci. 75, 716–718]. In this mechanism, rotation of the c-subunit was conceived to take place in 12 discrete steps of 30° each due to the binding and unbinding of protons to/from the leading and trailing Asp-61 residues of the c-subunit, respectively. Based on this molecular mechanism, a kinetic scheme has been developed in this work. The scheme considers proton transport driven by a concentration gradient of protons across the proton half-channels, and the rotation of the c-subunit by changes in the electrical potential only. This kinetic scheme has been analyzed mathematically and an expression has been obtained to explain the pH dependence of the rate of ATP synthesis by ATP synthase under steady state operating conditions. For a single set of three enzymological kinetic parameters, this expression predicts the rates of ATP synthesis which agree well with the experimental data over a wide range of pH_{in} and pH_{out}. A logical consequence of our analysis is that ΔpH and $\Delta\psi$ are kinetically inequivalent driving forces for ATP synthesis.

Key words: ATP synthase; Kinetic model; Torque; pH; Electrical potential; Energy transduction; Inequivalence; Kinetic parameter

1. Introduction

Adenosine triphosphate synthase (ATP synthase or F_1F_0ATPase) is the universal enzyme in biological energy conversion that is present in the membranes of mitochondria, chloroplasts and bacteria with an amazingly similar structure and function in different species. It synthesizes ATP from ADP and inorganic phosphate using the energy of a transmembrane electrochemical gradient of protons or Na^+ ions. This large enzyme complex has an overall molecular weight of 520 000 in *Escherichia coli* and consists of two major parts: a membrane-extrinsic, hydrophilic F_1 containing three α-, three β-, and one copy each of the γ-, δ- and ε-subunits, and a membrane-embedded, hydrophobic F_0 composed of one a-, two b- and 12 c-subunits. The F_0 and F_1 domains are linked by two slender stalks [1–6]. The central stalk is formed by the ε-subunit and part of the γ-subunit, while the peripheral stalk is constituted by the hydrophilic portions of the two b-subunits of F_0 and the δ-subunit of F_1. The ion channel is formed by the interacting regions of a- and c-subunits in F_0, while the catalytic binding sites are predominantly in the β-subunits of F_1 at the α–β interface [1–5]. The molecular mechanism of coupling ion translocation through F_0 to ATP synthesis in F_1 is unknown.

According to Mitchell's chemiosmotic theory [7,8], the electrochemical potential difference, $\Delta\mu_H$, developed during respiration and photosynthesis consists of two distinct parameters, an electrical potential $\Delta\psi$ and a transmembrane concentration gradient of protons (ΔpH) that are related by the equation $\Delta\mu_H = \Delta\psi - (2.3RT/F)\Delta pH$. Energetic equivalence of ΔpH and the electrical potential at equilibrium are an essential feature of the chemiosmotic theory. Almost 35 years ago, in a classical experiment using the acid bath procedure on chloroplast ATP synthase, it was reported that ATP synthesis is driven entirely by ΔpH [9]. However, recent experiments demonstrate that in the chloroplast ATP synthase, as well as in the mitochondrial and bacterial enzyme, the electrical potential is a mandatory driving force for ATP synthesis [10–12], and the electrical potential induces a rotary torque in the F_0 portion of *Propionigenium modestum* ATP synthase [12]. Thus, both ΔpH and $\Delta\psi$ are required for ATP synthesis. We had proposed the first molecular mechanism of torque generation in the F_0 portion of ATP synthase that considers the role of both ΔpH and $\Delta\psi$ and in particular addresses the indispensable requirement of the electrical potential for ATP synthesis [13].

Different models have been proposed for ion translocation and torque generation in ATP synthase [13–18]. In one class of models, the ring of c-subunits moves in a directed way as a result of Brownian rotational fluctuations [15,16]; in fact, electrostatic forces oppose the motion of the c-rotor [16]. In another model [14], the formation and breaking of a hydrogen bond leads to rotation of the c-subunit. In these models, ΔpH acts as the principal driving force for rotation, and therefore for ATP synthesis also. In another class of models [17,18], the role of the electrical potential is taken into account. Thus, the Na^+ ions are envisaged to be driven by the electrical potential from the periplasm through a stator channel into a specific binding site, thereby causing rotation of the rotor [17]. These models [14–17] are not compatible with the roles of both components of the electrochemical potential gradient. In our mechanism [13], the roles of both ΔpH and $\Delta\psi$ are highlighted, and torque generation in the F_0 portion of ATP synthase is a result of change in electrostatic potential brought about by the ion gradient.

In this paper, a kinetic model to predict the variation of the rate of ATP synthesis as a function of ΔpH (or $\Delta\mu_H$, for a

*Corresponding author. Fax: (91)-11-6868521.
E-mail: sunath@dbeb.iitd.ernet.in

0014-5793/00/$20.00
PII: S0014-5793(00)01716-6

certain steady state value of $\Delta\psi$) is developed. The model is based on our proposed molecular mechanism of torque generation in ATP synthase [13]. The developed kinetic scheme considers the mode of functioning of a single molecule; however, our mathematical analysis is applicable to a population of molecules. The model is compared to experimental data [19] and is found to be consistent with it for a wide range of pH_{in} and pH_{out} values.

2. Kinetic scheme for the molecular mechanism

The c-subunit, which functions as the rotor, has Asp-61 as the essential amino acid in each of its subunits [14,20]. Arg-210 and His-245 are the key amino acids in the a-subunit [14,21], which acts as the stator (the residue numbers for the F_0 domain refer to *E. coli*). The exact spatial orientation of these charges is unknown and Fig. 1 represents a possible geometry that can lead to generation of a unidirectional torque. The geometry of the a- and c-subunits is such that while c is a complete cylinder, the a-subunit is part of a cylinder coaxial to c, covering two subunits of c.

The negatively charged Asp-61 must be protonated when exposed to the membrane and unprotonated at the a–c interface. When both Asp-61 residues are unprotonated, the system is at equilibrium. The proton concentration at the inner membrane, H^+_{in}, is higher than the proton concentration, H^+_a in the vicinity of the leading Asp-61 residue across the proton half-channel. This concentration gradient drives the proton through the half-channel, causing it to bind to the leading Asp-61 residue. Now the positively charged His-245 attracts the trailing unprotonated Asp-61, disturbing the equilibrium and causing the inner cylinder to rotate (Fig. 1). Thus the leading Asp-61 moves into the membrane and a new protonated Asp-61 enters the interface. Rotation in the reverse direction is prevented by the large free energy barrier to transport an unprotonated Asp-61 from the interface into the hydrophobic membrane environment. When a new protonated Asp-61 residue enters the interface, it loses its proton to become unprotonated. The proton concentration in the vicinity of the trailing Asp-61 residue, H^+_b, is higher than the proton concentration in the matrix, H^+_{out}. As a result of this concentration gradient, the proton is driven out across the proton half-channel facing the matrix (Fig. 1). The proton gradient causes a change in electrostatic potential resulting in torque generation in the F_0 portion of ATP synthase. Thus, rotation of the c-rotor is induced only by the electrical potential in our molecular mechanism of torque generation in ATP synthase. When the above molecular mechanism is expressed in the form of a sequence, we arrive at the kinetic scheme depicted in Fig. 2.

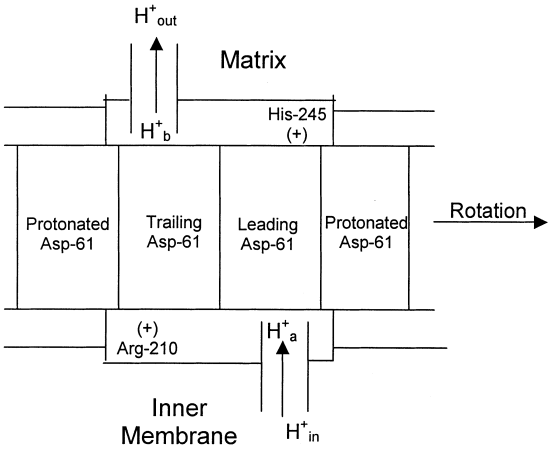

Fig. 1. Schematic diagram of a- and c-subunits of ATP synthase showing the path followed by the protons along with their concentrations.

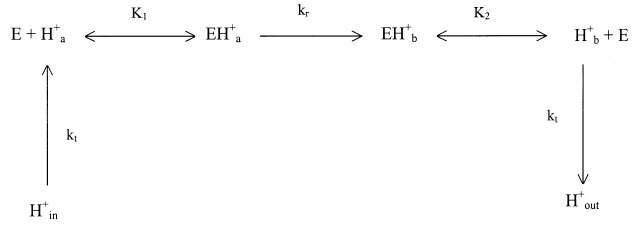

Fig. 2. Kinetic scheme based on the molecular mechanism of torque generation in ATP synthase.

In this kinetic scheme, E represents the ATP synthase enzyme molecule, EH^+_a the proton–enzyme complex before rotation of the c-rotor, and EH^+_b the proton–enzyme complex after the rotation. K_1 and K_2 denote the dissociation constants of the corresponding elementary steps (Fig. 2). k_r denotes the rate of conversion of EH^+_a to EH^+_b, i.e. it is a measure of the angular velocity of the c-rotor. k_t stands for the constant of proportionality relating the rate of proton transfer across the two proton half-channels to the corresponding proton concentration gradients (Fig. 2).

3. Mathematical analysis of the kinetic scheme

For steady state operation, the rates of proton transport, binding and dissociation, and rotation of the c-rotor are equal. Thus, v_{rot}, the rate of rotation of the c-subunit, can be written as

$$v_{rot} = k_t(H^+_{in} - H^+_a) \quad (1)$$

$$v_{rot} = k_r EH^+_a \quad (2)$$

and

$$v_{rot} = k_t(H^+_b - H^+_{out}) \quad (3)$$

From the material balance on E, we have

$$E_0 = E + EH^+_a + EH^+_b \quad (4)$$

where E_0 represents the total enzyme concentration. Thus,

$$E_0 = E + EH^+_a/K_1 + EH^+_b/K_2 \quad (5)$$

i.e.

$$E = E_0/\{1 + H^+_a/K_1 + H^+_b/K_2\} \quad (6)$$

Combining Eqs. 2 and 6, we have

$$v_{rot} = k_r E_0 H^+_a/\{K_1 + H^+_a + H^+_b(K_1/K_2)\} \quad (7)$$

Expressing H_a^+ and H_b^+ in terms of H_{in}^+ and H_{out}^+ using Eqs. 1 and 3 leads to

$$v_{rot} = (k_r E_0)(H_{in}^+ - v_{rot}/k_t)/[K_1 + H_{in}^+ + H_{out}^+(K_1/K_2) + v_{rot}\{(K_1/K_2) - 1\}/k_t] \quad (8)$$

The rate of ATP synthesis is proportional to the rate of rotation of the c-subunit, provided that substrate is available in the F_1 portion of ATP synthase, i.e.

$$v_{syn} = k_s v_{rot} \quad (9)$$

For very fast diffusion of protons into and from the F_0 portion across the proton half-channels, i.e. for k_t very large, we obtain on combining Eqs. 8 and 9

$$v_{syn} = (k_s k_r E_0) H_{in}^+ / [H_{in}^+ + H_{out}^+(K_1/K_2) + K_1 + k_r E_0/k_t] \quad (10)$$

which is the principal result of our mathematical analysis. Dividing the numerator and the denominator of Eq. 10 by H_{out}^+, we can analyze the dependence of v_{syn} with respect to ΔpH, or with respect to pH_{out} at a particular value of pH_{in}. Thus,

$$v_{syn} = (k_s k_r E_0)(H_{in}^+/H_{out}^+)/[(H_{in}^+/H_{out}^+) + (K_1/K_2) + (K_1 + k_r E_0/k_t)/H_{out}^+] \quad (11)$$

Eq. 10 can be rearranged to obtain the form

$$v_{syn} = V_{max} H_{in}^+ / [H_{in}^+ + K_m'] \quad (12)$$

where

$$K_m' = K_m(1 + H_{out}^+/K_I)$$

$$V_{max} = k_s k_r E_0$$

$$K_m = K_1 + k_r E_0/k_t$$

and

$$K_I = K_2[1 + k_r E_0/(K_1 k_t)]$$

4. Results and discussion

The rate of ATP synthesis shows a Michaelis–Menten type hyperbolic dependence with respect to H_{in}^+, as can be clearly inferred from Eq. 10. Further, inspection of Eq. 11 indicates that the rate of ATP synthesis follows a Michaelis–Menten type of dependence on the activity ratio, H_{in}^+/H_{out}^+. This is entirely consistent with recent experimental observations on the influence of the activity ratio on the rate of ATP synthesis [22]. A plot of v_{syn} (calculated using Eq. 10) as a function of $-pH_{in}$ yields a sigmoidal relationship. Similarly, a sigmoidal relationship is obtained for the rate of ATP synthesis (i.e. v_{syn} using Eq. 11) as a function of ΔpH or with respect to pH_{out} for a particular value of pH_{in}.

Detailed experiments to study the dependence of the rate of ATP synthesis on pH_{in}, pH_{out} and ΔpH have been carried out on ATP synthase from various sources such as chloroplasts [19,23], and *E. coli* [23]. Thus, the relative rate of ATP synthesis (v_{syn}/v_{st}) has been measured as a function of pH_{in} as well as ΔpH for a wide range of pH_{out} values for the chloroplast ATP synthase [19]. The relative rate of ATP synthesis has also been plotted as a function of pH_{out} at five different values of pH_{in}. Standard rates (v_{st}) were measured for each set of experiments (constant pH_{out}, different values of pH_{in}) under the same conditions with pH_{out} 8.5 and pH_{in} 5.1 [19]. Based on these experimental data, we have determined the best-fit values of the three parameters, $k_s k_r E_0$, K_1/K_2 and $(K_1 + k_r E_0/k_t)$, appearing in Eq. 11 of our kinetic model. The values of these parameters are given in Table 1. Based on Eqs. 10 and 11 of our kinetic model and these parameter values, the relative rate of ATP synthesis has been plotted as a function of pH_{in}, ΔpH and pH_{out} in Fig. 3a–c, respectively. These

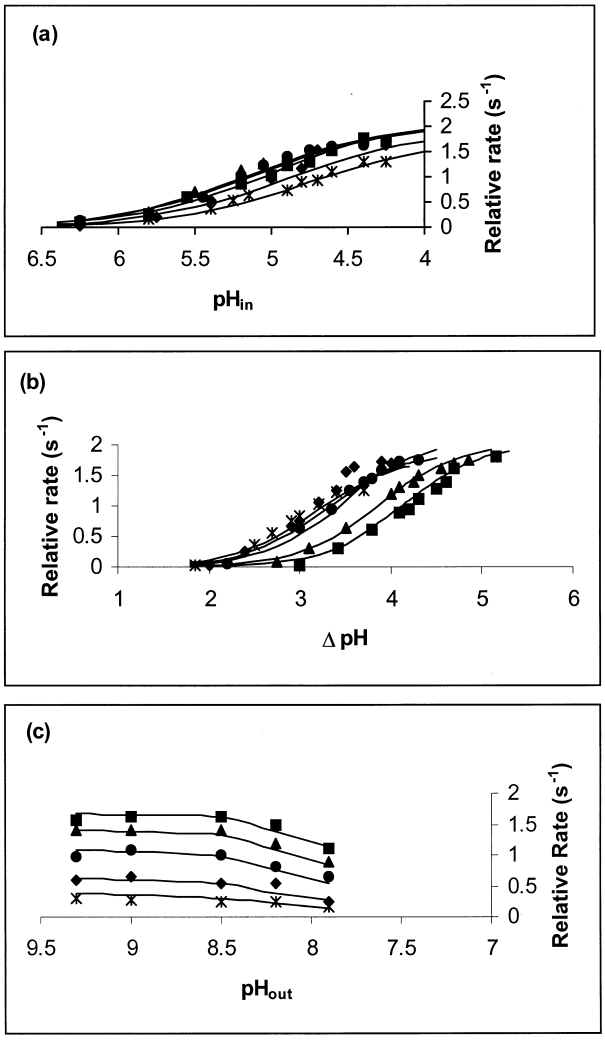

Fig. 3. Relative rates of ATP synthesis as a function of (a) pH_{in}; (b) ΔpH; (c) pH_{out}. Bold lines represent calculated rates using Eqs. 10 and 11 of our kinetic model and the parameter values given in Table 1. Points represent experimental data [19]: (a) pH_{out} 9.3 (■); pH_{out} 9.0 (▲); pH_{out} 8.5 (●); pH_{out} 8.2 (♦); pH_{out} 7.9 (*); (b) pH_{out} 9.3 (■); pH_{out} 9.0 (▲); pH_{out} 8.5 (●); pH_{out} 8.2 (♦); pH_{out} 7.9 (*); (c) pH_{in} 4.5 (■); pH_{in} 4.8 (▲); pH_{in} 5.1 (●); pH_{in} 5.5 (♦); pH_{in} 5.8 (*).

Table 1
Parameter values for Eqs. 10 and 11 obtained for the experimental data on the pH dependence of ATP synthesis [19]

Parameter	Value
$k_s k_r E_0$	57 s^{-1}
K_1/K_2	900
$K_1+k_r E_0/k_t$	$10^{-5.18}$ M

computed rates of ATP synthesis are found to agree well with the experimental data over the entire range (pH_{out} 7.9–9.3) for the same set of parameter values. It is all the more interesting to note that this agreement between theory and experiment is obtained even though the values of the standard rates of ATP synthesis change substantially in the course of the experiments.

Eq. 12 obtained by rearrangement of Eq. 10 contains V_{max}, K_m and K_I as the enzymological kinetic parameters which can all be experimentally determined. These enzymological kinetic parameters can be expressed in terms of the above-mentioned set of three parameter values (Table 1), as shown by Eq. 12 of our kinetic model. This implies that the parameters have biological significance attached to them. The values of these enzymological kinetic parameters for chloroplast ATP synthase from our kinetic model are tabulated in Table 2. Eq. 12 of our kinetic model suggests the occurrence of competitive inhibition of ATP synthase by H^+_{out} as the inhibitor in the synthesis mode. This implies that H^+_{out} competes with H^+_{in}, or the H^+_b bound to the trailing Asp-61 residue changes the conformation of the leading Asp-61 residue, which is the binding site for the H^+_a, thereby not allowing H^+_a to bind to the leading Asp-61 residue. Hence, unless H^+_b is released from the trailing Asp-61 residue, binding of H^+_a is not possible. Thus, for the physiological mode of steady state ATP synthesis, H^+_b unbinding and subsequent release must precede H^+_a binding. Thus, an order is imposed on binding and release events in the F_0 portion of the ATP synthase.

From Table 1, we see that the ratio of the dissociation constants, K_1/K_2, is high, which means that K_1 is high and/or K_2 is low. This implies that H^+_a is high and H^+_b is low under operating conditions for ATP synthesis. In order to maintain the proton concentration gradient, H^+_{in} needs to be high and H^+_{out} needs to be low, i.e. $pH_{out} > pH_{in}$, which is indeed the case physiologically. This points to the fact that ATP synthesis is a regulated process. Had this not been the case, ATP synthesis would be possible even at low H^+_{in} and/or high H^+_{out}. This can also be inferred from Eq. 11; the maximum rate of ATP synthesis can be achieved at low H^+_{in} and/or high H^+_{out} (i.e. for a low value of H^+_{in}/H^+_{out}) for small values of K_1/K_2, which is not the physiological situation.

We have several comments on our kinetic model. Fig. 1 represents a possible charge geometry; however, our kinetic model can accommodate other charge geometries. Moreover, we are concerned primarily with the magnitude of the forces and not with the amino acid residues responsible for the generation of these forces; hence our analysis is very general and our results will not be affected by any modification in the spatial charge geometry. Further, this analysis is independent of the number of c-subunits in F_0; biochemical and genetic studies [24,25] as well as a thermodynamic analysis of ATP synthesis [26] suggest that the number of c-subunits is 12. However, a recent structural study suggests a ring with 10 c-subunits for ATP synthase from *Saccharomyces cerevisiae* mitochondria [27]. According to our kinetic scheme, these c-subunits undergo a full and unidirectional rotation. Although we have focused on the pH dependence of the rate of ATP synthesis, our kinetic model is also applicable to the dependence of the ATP synthesis rate on the electrochemical potential difference because our analysis is based on steady state considerations for a constant value of the electrical potential. The required equation can be readily obtained by substituting for the activity ratio by the electrochemical potential difference using Mitchell's chemiosmotic equation (see Section 1) in Eq. 11. Finally, it is not correct to say that our kinetic model is entirely based on proton concentrations; in fact, since all the three enzymological kinetic parameters depend on k_r (Eq. 12), which itself is a function of $\Delta\psi$, the rate of ATP synthesis is based on both ΔpH and $\Delta\psi$.

Table 2
Enzymological kinetic parameters for Eq. 12 obtained for the experimental data on the pH dependence of ATP synthesis [19]

Kinetic parameter	Value
V_{max}	57 s^{-1}
K_m	6.6×10^{-6} M
K_I	7.3×10^{-9} M

A similar equation is applicable to ATP hydrolysis provided H^+_{in} and H^+_{out} refer to the proton concentrations in the matrix and inner membrane, respectively, and the labels 'leading' and 'trailing' of the Asp-61 residues are interchanged (with H^+_a and H^+_b associated with the above leading and trailing Asp-61 residues). This ensures that protons are translocated from the matrix to the inner membrane during ATP hydrolysis. Though K_1 and K_2, the dissociation constants of the corresponding elementary steps (Fig. 2), remain the same, however, depending on the distances between the stator–rotor charges and the environment, k_r may not be the same in the hydrolysis and synthesis modes of operation.

A major consequence of our kinetic scheme is that the two components of the electrochemical potential difference, ΔpH, and $\Delta\psi$ (through k_r) act at different elementary steps in our molecular mechanism for torque generation by F_0 (Figs. 1 and 2), and each component can affect the rate of ATP synthesis independent of each other. In fact, k_r is a function of $\Delta\psi$, and any change in $\Delta\psi$ alters the rate of ATP synthesis by changing the rate constant k_r independently of the way a change in ΔpH affects the rate of ATP synthesis. This can also be seen from Eqs. 10 and 11 and Fig. 3. For very high values of ΔpH, the rate of ATP synthesis reaches a saturation value; however, changing the value of $\Delta\psi$ changes k_r, which in turn alters the rate of ATP synthesis. This indicates that ΔpH and $\Delta\psi$ are kinetically inequivalent driving forces for ATP synthesis. A mathematical analysis of the relation between $\Delta\psi$ and ΔpH is currently being prepared for publication (Jain and Nath, in preparation).

5. Conclusions

Based on a novel molecular mechanism of torque generation in ATP synthase, a kinetic model has been developed, analyzed and compared with experimental data on the pH dependence of the rate of ATP synthesis. The kinetic scheme takes into account the roles of ΔpH and $\Delta\psi$ in proton transport and rotation of the c-subunit in the F_0 portion of ATP

synthase. Rotation of the c-rotor is driven only by $\Delta\psi$ in our kinetic scheme. The model agrees well with experimental data; in fact, a single set of three enzymological kinetic parameters, V_{max}, K_m and K_I, is found to be consistent with the experimental data over the entire range of pH. Our kinetic model imposes an order on binding and release events. An important consequence of our model is that ΔpH and $\Delta\psi$ are kinetically inequivalent in driving ATP synthesis.

Acknowledgements: S.N. thanks the Department of Science and Technology, India and the All India Council of Technical Education for financial support.

References

[1] Abrahams, J.P., Leslie, A.G.W., Lutter, R. and Walker, J.E. (1994) Nature 370, 621–628.
[2] Shirakihara, Y., Leslie, A.G.W., Abrahams, J.P., Walker, J.E., Ueda, T., Sekimoto, Y., Kambara, M., Saika, K., Kagawa, Y. and Yoshida, M. (1997) Structure 5, 825–836.
[3] Boyer, P.D. (1997) Annu. Rev. Biochem. 66, 717–749.
[4] Weber, J. and Senior, A.E. (1997) Biochim. Biophys. Acta 1319, 19–57.
[5] Zhou, Y., Duncan, T.M. and Cross, R.L. (1997) Proc. Natl. Acad. Sci. USA 94, 10583–10587.
[6] Wilkens, S. and Capaldi, R.A. (1998) Nature 393, 29.
[7] Mitchell, P. (1961) Nature 191, 144–148.
[8] Mitchell, P. (1966) Biol. Rev. 41, 445–502.
[9] Jagendorf, A.T. and Uribe, E. (1966) Proc. Natl. Acad. Sci. USA 55, 170–177.
[10] Kaim, G. and Dimroth, P. (1998) FEBS Lett. 434, 57–60.
[11] Kaim, G. and Dimroth, P. (1999) EMBO J. 18, 4118–4127.
[12] Kaim, G. and Dimroth, P. (1998) EMBO J. 17, 5887–5895.
[13] Rohatgi, H., Saha, A. and Nath, S. (1998) Curr. Sci. 75, 716–718.
[14] Vik, S.B. and Antonio, B.J. (1994) J. Biol. Chem. 269, 30364–30369.
[15] Cherepanov, D.A., Mulkidjanian, A.Y. and Junge, W. (1999) FEBS Lett. 449, 1–6.
[16] Elston, T., Wang, H. and Oster, G. (1998) Nature 391, 510–513.
[17] Dimroth, P., Kaim, G. and Matthey, U. (1998) Biochim. Biophys. Acta 1365, 87–92.
[18] Dimroth, P., Wang, H., Grabe, M. and Oster, G. (1999) Proc. Natl. Acad. Sci. USA 96, 4924–4929.
[19] Possmayer, F.E. and Gräber, P. (1994) J. Biol. Chem. 269, 1896–1904.
[20] Fraga, D., Hermolin, J. and Fillingame, R.H. (1994) J. Biol. Chem. 269, 2562–2567.
[21] Eya, S., Maeda, M. and Futai, M. (1991) Arch. Biochem. Biophys. 284, 71–77.
[22] Pänke, O. and Rumberg, B. (1999) Biochim. Biophys. Acta 1412, 118–128.
[23] Fischer, S. and Gräber, P. (1999) FEBS Lett. 457, 327–332.
[24] Jones, P.C., Jiang, W. and Fillingame, R.H. (1998) J. Biol. Chem. 273, 17178–17185.
[25] Jones, P.C. and Fillingame, R.H. (1998) J. Biol. Chem. 273, 29701–29705.
[26] Nath, S. (1998) Pure Appl. Chem. 70, 639–644.
[27] Stock, D., Leslie, A.G.W. and Walker, J.E. (1999) Science 286, 1700–1704.